Statistical Capacity Analysis of Converged Metro-Access Optical Networks for 6G Any-Haul

(Article begins on next page)

Statistical Capacity Analysis of Converged Metro-Access Optical Networks for 6G Any-Haul

Ahtisham Ali[1,2], Muhammad Umar Masood[2], Sanwal Zeb[2], Riccardo Schips[2], Andrea Rosso[2], Gulmina Malik[2], Bruno Correia[3], Alessandro Galardini[1], Vittorio Curri[2]

[1]Consorzio TOP-IX, Via Maria Vittoria N 38, 10123 Torino, Italy
[2]Department of Electronics and Telecommunications, Politecnico di Torino, Corso Duca degli Abruzzi 24, 10129 Torino, Italy
[3]Nokia, Optical Networks, Rua da Garagem 1, 2790-078, Carnaxide, Portugal

Author e-mail address: ahtisham.ali@top-ix.org

Abstract: *We present a Monte Carlo statistical analysis of transport capacity in converged metro-access optical networks for 6G RAN traffic, showing spectral granularity limits single-carrier systems, while DSCM enables finer allocation and order-of-magnitude capacity gains.*

Keywords: *Optical fronthaul and backhaul, Optical metro and core networks, Optical communication systems*

I. Introduction

Global mobile traffic is expected to continue its rapid growth, driven by emerging 6G services and data-intensive applications, further increasing the pressure on transport network infrastructures [1–3]. In parallel, disaggregated and open radio access network (RAN) architectures enable flexible placement of radio units (RUs), distributed units (DUs), and centralized units (CUs) across geographically distributed locations, bringing programmability and deployment agility [4]. Each RU requires a transport bit rate of approximately 22.2 Gbps, considering functional split 7.2 by 3GPP, to be supported over the fronthaul (FH) and midhaul (MH) segments with latency budgets on the order of 250 µs and 1 ms, respectively [5–8]. These aspects have already been investigated in converged metro-access networks through route-level feasibility studies under joint physical layer and latency constraints, highlighting the role of functional placement and transmission technologies [9–11].

Meanwhile, optical infrastructure in metro networks is already deployed and is being shared among multiple services, with residual C-band capacity typically available. This available spectrum can be leveraged under a spectrum as-a-service to support RAN traffic, enabling dynamic allocation of resources over shared infrastructure. However, efficiently utilizing such available spectrum for fine-granular and latency-constrained RAN traffic requires careful consideration of both resource allocation and physical-layer feasibility.

Conventional single-carrier (SC) transmission limits its ability to efficiently accommodate moderate-rate RAN demands. In contrast, digital subcarrier multiplexing (DSCM) provides improved matching between transport resources and RU-level traffic granularity [12, 13]. This becomes increasingly critical under RU densification, where the growing number of RUs intensifies the demand on limited spectral resources and directly impacts the achievable transport capacity.

Previous studies do not explicitly address the utilization of available spectral resources to support increasing RAN traffic demand under progressive network loading. In this work, we statistically investigate transport capacity in converged

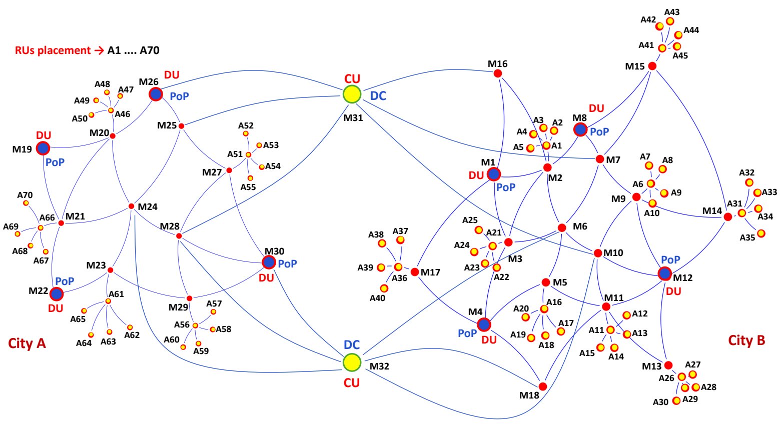

Topology Parameters

Parameter	City A	City B
Total optical nodes	44	63
Metro nodes	12	18
Access nodes	25	45
Avg. node degree	3.42	4.06
Avg. link length (km)	6.9	7.3
Max. span (km)	10	12
Max. FH hops (RU–DU)	4	
Max. MH hops (DU–CU)	8	

Fig. 1. Simulated converged metro-access network topology and corresponding parameters.

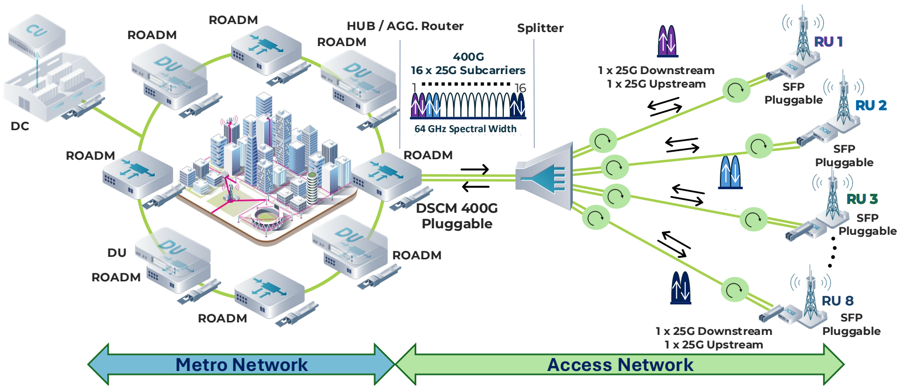

Fig. 2. Modeled Converged Metro Access Network Architecture

metro-access optical networks under joint physical-layer and latency constraints, motivated by the need to efficiently exploit available spectrum for latency-constrained RAN services. Extending the framework in [14] to metro-access scenarios and DSCM-based transmission, we quantify the supported traffic within a given spectral allocation using blocking probability (BP) as the primary performance metric. We further evaluate the impact of transmission configurations and analyze capacity scaling under increasing RU density, highlighting transport limits in spectrum-constrained metro environments. Results show that DSCM supports upto 8.8 Tbps at 10% residual C-band and 43.5 Tbps at 40% within a BP of 1%.

II. Network Architecture and Modeling

The performance evaluation is conducted on a representative converged metro-access optical network (Fig. 1), spanning two metropolitan areas comprising access and metro segments, reflecting a realistic operator-grade deployment [8]. Access nodes (A-nodes) correspond to RUs, while metro nodes (M-nodes) are modeled as reconfigurable Optical Add-Drop Multiplexers (ROADMs) enabling traffic aggregation within the optical layer. Each access cluster consists of four access nodes connected to the metro network via circulators, a splitter, and a ROADM, emulating bidirectional (BiDi) access and dual-fiber operation as shown in Fig. 2. DU functionalities are hosted at selected metro nodes, whereas CU functions are centralized at data centers located at nodes M31 and M32, forming RU–DU–CU (end-to-end, E2E) paths across FH and MH segments.

Physical-layer performance is evaluated using a Python-based framework built on GNPy [15, 16], enabling modeling of fiber attenuation, amplified spontaneous emission (ASE) noise, and nonlinear interference (NLI). All links are assumed to be standard single-mode fiber (SSMF) with attenuation 0.25 dB/km, and EDFAs with a 6 dB noise figure. Node impairments include a circulator loss of 0.81 dB at the access interface and a ROADM insertion loss of 10 dB at metro nodes [10, 17].

Transmission performance is captured using experimentally characterized models of SC and DSCM pluggable transceivers, providing a mapping between received optical power (ROP) and signal-to-noise ratio (SNR). The end-to-end SNR is computed as $\mathrm{SNR}^{-1} = \mathrm{GSNR}^{-1} + \mathrm{SNR}_{\mathrm{TRx}}^{-1}$, and the corresponding bit-error-rate (BER) as $\mathrm{BER} = k_1 \,\mathrm{erfc}\left(\sqrt{k_2 \cdot \mathrm{SNR}}\right)$, with a feasibility threshold of 10^{-2}, consistent with hard-decision pre-FEC limits [18, 19]. Latency is evaluated from propagation delay assuming $5\,\mu\mathrm{s\,km}^{-1}$ for SSMF, while transceiver processing delays are neglected, as they are comparatively negligible in transparent optical transport scenarios [20].

Network performance is assessed via Monte Carlo (MC) simulations with 1000 independent iterations. Traffic demands are progressively generated and mapped onto E2E paths, and each request is evaluated under joint GSNR, BER, and latency constraints. If a feasible route and spectrum assignment cannot be identified, the request is blocked. This process enables the characterization of network capacity as a function of offered load, using BP as the primary performance metric. The overall workflow is summarized in Fig. 3, where routing, physical-layer evaluation, and spectrum allocation are performed iteratively for each demand.

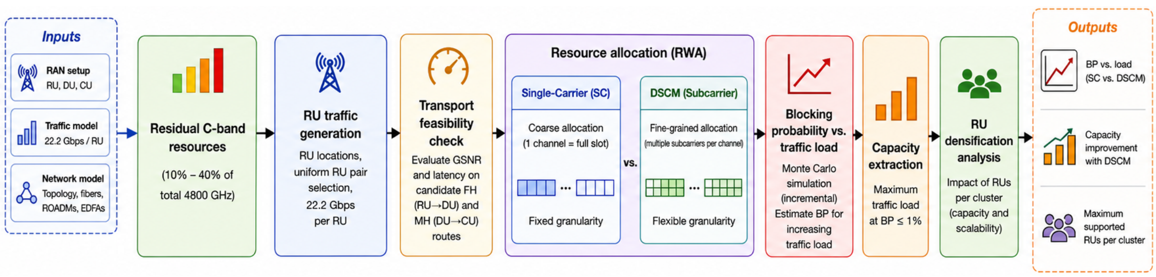

Fig. 3. Simulation Workflow

III. Results and Discussion

Fig. 4a shows the BP as a function of offered RAN traffic load for different levels of available C-band spectrum with a channel-width of 75 GHz and DP-16QAM. As expected, increasing the available spectrum extends the supported load region, shifting the operating point toward higher traffic volumes before the BP reaches 1%. A clear performance gap between SC and DSCM transmission is observed. For the same spectral allocation, DSCM sustains significantly higher traffic loads compared to SC, reflecting its ability to more efficiently utilize the available spectrum through fine-granular allocation. This difference becomes more pronounced at higher loads, where resource constraints dominate and efficient spectrum usage is critical.

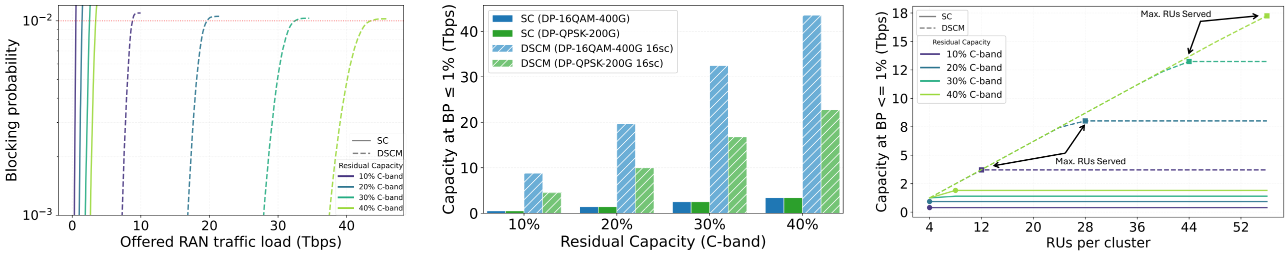

(a) (b) (c)

Fig. 4. Performance evaluation under different residual C-band capacity scenarios: (a) blocking probability versus offered load for SC and DSCM schemes; (b) network capacity at 1% blocking probability as a function of available residual C-band capacity for different transmission schemes; (c) impact of RU density on supported capacity at 1% blocking probability.

Fig. 4b quantifies the achievable network capacity at a BP of 1% for different transmission configurations. For SC transmission, both DP-QPSK and DP-16QAM achieve identical capacity values across all spectrum allocations (e.g., 0.5 Tbps at 10% C-band and 3.4 Tbps at 40%), indicating that system performance is primarily limited by spectrum availability rather than modulation format. In this regime, the coarse channel granularity dominates, masking the benefits of higher spectral efficiency. In contrast, DSCM provides a substantial capacity increase across all configurations. For example, at 10% C-band, DSCM with DP-16QAM achieves approximately 8.8 Tbps, compared to 0.5 Tbps for SC, corresponding to more than an order-of-magnitude improvement. This gain persists across all spectrum allocations, reaching up to 43.5 Tbps at 40% C-band. Even with lower-order modulation (DP-QPSK), DSCM significantly outperforms SC, confirming that the dominant factor is the improved granularity of spectrum allocation rather than modulation efficiency alone. These results highlight that, under moderate-rate RAN traffic demands, efficient resource matching enabled by DSCM is more impactful than increasing per-channel spectral efficiency.

Fig. 4c shows the supported network capacity at a BP of 1% as a function of the number of RUs per access cluster for DP-16QAM. For SC transmission, the achievable capacity remains essentially constant regardless of RU density (e.g., 0.4–1.9 Tbps depending on spectrum allocation), indicating that the system is constrained by fixed channel granularity and cannot effectively exploit additional traffic aggregation.

In contrast, DSCM exhibits a strong dependence on RU density. As the number of RUs per cluster increases, the supported capacity grows significantly, particularly for higher spectrum allocations. For instance, at 40% C-band, the supported capacity increases from approximately 1.2 Tbps at 4 RUs per cluster to over 17 Tbps at 56 RUs per cluster. This behavior reflects the ability of DSCM to aggregate multiple moderate-rate RU demands efficiently through subcarrier-level allocation. Moreover, the results show that the capacity scaling saturates beyond a certain RU density, particularly under limited spectrum (e.g., 10% and 20% C-band), where the system becomes resource-limited. This saturation indicates the fundamental transport limits imposed by available spectrum under joint physical-layer and latency constraints.

IV. Conclusion

This work evaluated the transport capacity of converged metro-access optical networks for RAN traffic under joint physical-layer and latency constraints. The results show that SC transmission is limited by fixed channel granularity, leading to inefficient utilization of available spectrum. In contrast, DSCM enables fine-granular resource allocation, increasing supported capacity from 0.5 to 8.8 Tbps at 10% residual C-band and from 3.4 to 43.5 Tbps at 40%. Furthermore, DSCM supports a capacity exceeding 17 Tbps under RU densification. These results confirm that efficient matching between traffic granularity and spectral resources, rather than spectral efficiency alone, is the key factor in maximizing transport capacity, highlighting DSCM as a promising solution for future 6G x-haul networks.

Acknowledgment

Ahtisham Ali's work is fully funded by the European Union's Horizon 2020 research and innovation programme under the Marie Skłodowska-Curie project EWOC under GA No. 101073265. This work has also received support from the MSCA project NESTOR under GA No. 101119983, the EU Horizon Project ALLEGRO GA No. 101092766, and the PNRR-NGEU (MUR–DM117/2023).

REFERENCES

[1] C.-X. Wang, X. You, X. Gao, X. Zhu, Z. Li, C. Zhang, H. Wang, Y. Huang, Y. Chen, H. Haas, J. S. Thompson, E. G. Larsson, M. D. Renzo, W. Tong, P. Zhu, X. Shen, H. V. Poor, and L. Hanzo, "On the road to 6g: Visions, requirements, key technologies, and testbeds," *IEEE Communications Surveys & Tutorials*, vol. 25, no. 2, pp. 905–974, 2023.

[2] P. A. Baziana, "Optical data center networking: A comprehensive review on traffic, switching, bandwidth allocation, and challenges," *IEEE Access*, vol. 12, pp. 186 413–186 444, 2024.

[3] Ericsson, "Mobile traffic forecasts, ericsson mobility report," Tech. Rep., 2025, accessed: 2025-08-29. [Online]. Available: https://www.ericsson.com/en/reports-and-papers/mobility-report/dataforecasts/mobile-traffic-forecast

[4] A. Tzanakaki, M. Anastasopoulos, V. Alevizaki, and A. Manolopoulos, "Optical networking in support of 5g and 6g infrastructures," in *2025 International Conference on Optical Network Design and Modeling (ONDM)*, 2025, pp. 1–3.

[5] 3GPP, "Study on CU-DU lower layer split for NR; (release 15)," 3GPP, Tech. Rep. TR 38.816 V15.0.0 (2017-12), 2017.

[6] PROTEUS-6G Consortium, "D2.1: 6G x-haul network requirements," PROTEUS-6G Project, EU Horizon Europe, Tech. Rep., 2024. [Online]. Available: https://proteus-6g.eu/wp-content/uploads/2025/11/PROTEUS-6G_D2.1_6G_x-haul_network_requirements.pdf

[7] A. Tzanakaki, M. Anastasopoulos, and V.-M. Alevizaki, "Optical transport networks converging edge compute and central cloud: An enabler for 6g services," in *2024 Optical Fiber Communications Conference and Exhibition (OFC)*, 2024, pp. 1–3.

[8] A. Ali, S. Zeb, A. Rosso, M. U. Masood, G. Malik, R. Ambrosone, R. Schips, B. Correia, S. Straullu, F. Aquilino, J. Pedro, A. Napoli, A. Galardini, and V. Curri, "Optimizing ran x-haul performance through targeted hollow-core fiber deployment in converged metro-access networks," in *2025 International Conference on Software, Telecommunications and Computer Networks (SoftCOM)*, 2025, pp. 1–6.

[9] A. Ali, S. Zeb, A. Rosso, M. U. Masood, G. Malik, R. Ambrosone, R. Schips, S. Straullu, F. Aquilino, J. Pedro, A. Napoli, A. Galardini, and V. Curri, "Evaluating metro-access optical networks as-a-service for flexible ran x-haul," in *2025 IEEE Conference on Standards for Communications and Networking (CSCN)*, 2025, pp. 1–6.

[10] A. Ali, M. U. Masood, A. Rosso, G. Malik, M. Pollone, A. Galardini, and V. Curri, "Statistical analysis of end-to-end route feasibility in converged metro–access optical networks," *IEEE Photonics Technology Letters*, pp. 1–1, 2026.

[11] A. Ali, M. U. Masood, S. Zeb, A. Rosso, G. Malik, R. Schips, R. Ambrosone, S. Straullu, A. Nespola, B. Correia, J. Pedro, A. Napoli, A. Galardini, and V. Curri, "Benefits of selective hollow-core fiber deployment for 6g x-haul in converged metro-access networks," in *2026 International Conference on Optical Network Design and Modeling (ONDM)*, 2026, accepted.

[12] D. Welch, A. Napoli, J. Bäck, S. Buggaveeti, C. Castro, A. Chase, X. Chen, V. Dominic, T. Duthel, T. A. Eriksson, S. Erkilinç, P. Evans, C. R. S. Fludger, B. Foo, T. Frost, P. Gavrilovic, S. J. Hand, A. Kakkar, A. Kumpera, V. Lal, R. Maher, F. Marques, F. Masoud, A. Mathur, R. Milano, M. I. Olmedo, M. Olson, D. Pavinski, J. Pedro, A. Rashidinejad, P. Samra, W. Sande, A. Somani, H. Sun, N. Swenson, H.-S. Tsai, A. Yekani, J. Zhang, and M. Ziari, "Digital subcarrier multiplexing: Enabling software-configurable optical networks," *Journal of Lightwave Technology*, vol. 41, no. 4, pp. 1175–1191, 2023.

[13] C. Castro, P. Torres-Ferrera, M. Sezer Erkilinc, J. Sime, G. Parisi, J. Pedro, M. Quagliotti, M. Porrega, D. Hillerkuss, C. Fludger, E. Riccardi, and A. Napoli, "Power consumption considerations of coherent transceivers in filterless point-to-multipoint metro-aggregation networks with digital subcarrier multiplexing," *Journal of Optical Communications and Networking*, vol. 17, no. 6, pp. 526–542, 2025.

[14] V. Curri, M. Cantono, and R. Gaudino, "Elastic all-optical networks: A new paradigm enabled by the physical layer. how to optimize network performances?" *Journal of Lightwave Technology*, vol. 35, no. 6, pp. 1211–1221, 2017.

[15] A. Ferrari, M. Filer, E. Le Rouzic, J. Kundrát, B. Correia, K. Balasubramanian, Y. Yin, G. Grammel, G. Galimberti, and V. Curri, "Gnpy: an open source planning tool for open optical networks," in *2020 International Conference on Optical Network Design and Modeling (ONDM)*, 2020, pp. 1–6.

[16] V. Curri, "Gnpy model of the physical layer for open and disaggregated optical networking [invited]," *Journal of Optical Communications and Networking*, vol. 14, no. 6, pp. C92–C104, 2022.

[17] R. Pennetta, M. Blaha, and A. Rauschenbeutel, "A low-loss and broadband all-fiber acousto-optic circulator," in *Frontiers in Optics*. Optica Publishing Group, 2024, pp. FW7D–4.

[18] T. Mano, A. D'Amico, Y.-K. Huang, G. Borraccini, H. Nishizawa, T. Wang, V. Curri, and K. Takasugi, "Measuring the transceiver's back-to-back ber-osnr characteristic using only a variable optical attenuator," in *ECOC 2024; 50th European Conference on Optical Communication*, 2024, pp. 1499–1502.

[19] A. Rosso, "Modeling and controlling optical transponder white-boxes based on the physical layer digital twin," Master's thesis, Politecnico di Torino, 2024. [Online]. Available: https://webthesis.biblio.polito.it/id/eprint/31825

[20] OpenZR+ MSA, "Openzr+: 400g digital coherent optics for multi-haul," https://openzrplus.org/resources/openzr-400g-digital-coherent-optics-for-multi-haul/, 2020, white paper.